Synthesis of Novel Biodegradable Thermoresponsive Triblock Copolymers Based on Poly[(R)-3-hydroxybutyrate] and Poly(N-isopropylacrylamide) and Their Formation of Thermoresponsive M...

ARTICLE *in* MACROMOLECULES · DECEMBER 2008

Impact Factor: 5.8 · DOI: 10.1021/ma8019865

Synthesis of Novel Biodegradable Thermoresponsive Triblock Copolymers Based on Poly[(*R*)-3-hydroxybutyrate] and Poly(*N*-isopropylacrylamide) and Their Formation of Thermoresponsive Micelles

Xian Jun Loh,[†,‡,§] Zhong-Xing Zhang,[†] Yun-Long Wu,[†] Tiong Soon Lee,[§] and Jun Li*[,†,‡,§]

*Division of Bioengineering, Faculty of Engineering, National University of Singapore (NUS), 7 Engineering Drive 1, Singapore 117574, Singapore, NUS Graduate School for Integrative Sciences and Engineering (NGS), 28 Medical Drive, Singapore 117456, Singapore, and Institute of Materials Research and Engineering, A*STAR (Agency for Science, Technology, and Research), 3 Research Link, Singapore 117602, Singapore*

Received September 4, 2008; Revised Manuscript Received October 21, 2008

ABSTRACT: Novel thermoresponsive amphiphilic triblock copolymers with two hydrophilic poly(*N*-isopropylacrylamide) blocks flanking a central hydrophobic poly[(*R*)-3-hydroxybutyrate] block were synthesized by atom transfer radical polymerization. The copolymers were characterized by gel permeation chromatography (GPC) and ^{1}H and ^{13}C NMR spectroscopy. The thermal stability of the copolymer was investigated by thermogravimetric analysis (TGA), and crystallization behavior was studied by differential scanning calorimetry (DSC). The water-soluble copolymers formed core−corona-type micelle aggregates in water. The critical micelle concentrations of the triblock copolymers were in the range of 1.5 to 41.1 mg/L, and the partition coefficients were in the range of (1.64−20.42) × 10^{5}. Transmission electron microscopy showed that the self-assembled micelle aggregates had well-defined spherical shape. The temperature sensitivity of the micelles was demonstrated by the phase transition of a 0.5 mg/mL aqueous polymer solution at the lower critical solution temperature (LCST). Preliminary cytotoxicity studies showed that these micelles were nontoxic and could be potential candidates for the encapsulation and release of therapeutic drugs in the biological system.

Introduction

Amphiphilic block copolymers have the ability to self-assemble into micelles in the aqueous medium and have been extensively investigated for their potential application in the nanomedicine and biomedical fields.[1−3] Micelles can be used as cleaning agents to extract pollutants from wastewater,[4] as template and structure control agents for materials synthesis,[5] as nanobioreactors in biotransformation processes,[6] or as phase-transfer catalysts.[7] The micelles have a hydrophobic core and hydrophilic corona, which interacts with the external aqueous environment. These micelles can aid in the aqueous solubilization of hydrophobic compounds and can act as nanocontainers of these compounds. As an example, micelles containing a hydrophobic drug can be injected into the human body. At the onset of injection, it is important that the micelles remain stable and not rupture under the sudden high dilution. Thus, having micelles with a low critical micelle concentration (CMC) is critical to its application.

Poly[(*R*)-3-hydroxybutyrate] (PHB) belongs to a class of biologically synthesized polyesters known as poly[(*R*)-3-hydroxyalkanoate]s.[8−13] PHB has been extracted from genetically modified plants.[14] PHB is a thermoplastic polyester with mechanical properties close to those of isotactic polypropylene, which can be extruded, molded, and spun using conventional processing equipment. Rising oil prices have seen the increasing popularity of the PHB compared with conventional commodity plastics. Because of its degradable nature, PHB is considered to be an environmentally friendly plastic when compared with its nondegradable counterparts such as polystyrene or polyethylene. These attractive properties have led to the use of PHB as materials in areas such as packaging. PHB degrades to D-3-hydroxybutyrate, which is a natural constituent of human blood.[15] As a result of this advantageous property, PHB may be suitable for a variety of biomedical applications, such as uses as drug carriers and tissue engineering scaffolds. Because of its inherent hydrophobicity, PHB is rarely used in applications that require good water solubility, such as polymeric micelles and gels. In 2003, our laboratory reported the synthesis of the first water-soluble PHB-based triblock copolymer.[3] These poly(ethylene oxide)-poly[(*R*)-3-hydroxybutyrate]-poly(ethylene oxide) (PEO-PHB-PEO) copolymers formed micelles that possess very good stability under high dilution conditions. More recently, our laboratory reported the first thermogelling copolymer based on PHB.[16−18] The advantage gained from using PHB in this case was that these PHB-based copolymers required very low concentrations in solution to exhibit the thermogelling behavior. This reduces the amount of polymer that is required in the preparation of an injectable formulation for drug release applications.[17]

Recently, thermosensitive micelles derived from poly(*N*-isopropylacrylamide) (PNIPAAm) have been reported.[19−24] PNIPAAm exhibits a lower critical solution temperature (LCST) of 32 to 33 °C, is hydrophilic at low temperatures, and precipitates above the critical phase-transition temperature. Block copolymers that compromise a hydrophobic segment such as poly(methyl methacrylate) (PMMA), poly(10-undecenoic acid), and poly(oleic acid) and hydrophilic PNIPAAm segments have been reported.[21−24] However, these thermoresponsive micelles are nondegradable, raising questions on the elimination of the micelles from the body after its use. The thermoresponsive

* Corresponding author: E-mail: bielj@nus.edu.sg. Tel: +65-6516-7273. Fax: +65-6872-3069.
† Division of Bioengineering, Faculty of Engineering, National University of Singapore (NUS).
‡ NUS Graduate School for Integrative Sciences and Engineering (NGS).
§ A*STAR (Agency for Science, Technology, and Research).

10.1021/ma8019865 CCC: $40.75
Published on Web 12/11/2008

poly(*N*-isopropylacrylamide-*co*-*N*,*N*-dimethylacrylamide) (PNIPAAm-PDMAAm) segments have been copolymerized with hydrophobic biodegradable segments such as poly(DL-lactic acid) (PDLLA), poly(lactic-co-glycolic acid) (PLGA), or PCL.[25−28] Biotinylated poly(*N*-isopropylacrylamide-*co*-*N*-(3-dimethylamino propyl)methacrylamide) has been copolymerized with PCL for cell tracking and drug delivery applications.[29] It was demonstrated that these micelles have a slow rate of drug release at temperatures below the critical phase-transition temperature but rapidly release encapsulated drug upon heating to above the critical phase-transition temperature. Triblock copolymers of PNIPAAm-PCL-PNIPAAm and PCL-PNIPAAm-PCL have been synthesized.[30,31] These copolymers show very low critical micellization concentrations in the range of 4−40 mg/L. The micelles obtained in both cases showed a spherical morphology seen on transmission electron microscopy (TEM) micrographs. The incorporation of the hydrophobic PCL segment does not appear to lower the LCST of the copolymer significantly. The synthesis of diblock copolymers of PNIPAAm and PDLLA were reported.[32] These diblock copolymers formed micelles in water. The authors found that when the length of the PDLLA segment was too long precipitates were obtained instead of micelles.

Here we report the synthesis of a new series of biodegradable thermoresponsive PNIPAAm-PHB-PNIPAAm triblock copolymers by atom transfer radical polymerization (ATRP). Our literature survey did not reveal any precedent reports on the synthesis and characterization of these copolymers. These triblock copolymers are expected to form thermoresponsive micelles that would be very stable under high dilution concentrations in the aqueous environment. These micelles can be made to release the contents held in the core upon exposure to a thermal stimulus, potentially allowing for thermally triggered drug release. To form micelles, the central PHB block must not be too long; otherwise, this would lead to water-insoluble block copolymers. During the design of the copolymers, we restricted the length of PNIPAAm blocks on either side of the PHB block to a molecular weight of <20 000 g/mol so as to allow the final degraded fragment to be easily excreted from the body via renal filtration. The renal excretion of PEG from the body system has been investigated.[33−35] For PEG with molecular weight of <30 000 g/mol, the elimination of the polymer was determined by molecular size and was removed from the body fairly rapidly. However, when the molecular weight of PEG was >30 000 g/mol, the polymers were excreted much more slowly by renal filtration. On the basis of the biodegradability and biocompatibility of the copolymers, these materials are excellent candidates for the encapsulation and delivery of hydrophobic drugs to the human body.

Experimental Section

Materials. Natural source PHB was purchased from Aldrich. The PHB sample was purified by dissolving in chloroform followed by filtration and precipitation in hexane before use. The M_n and M_w of the purified PHB are 8.7×10^4 and 2.3×10^5, respectively. Bis(2-methoxyethyl) ether (Diglyme, 99%), ethylene glycol (99%), dibutyltin dilaurate (95%), 2-bromoisobutyryl bromide (98%), *N*-isopropylacrylamide (NIPAAm, >99%), 1,1,4,7,10,10-hexamethyltriethylenetetramine (HMTETA, 99%), copper(I) bromide (CuBr, 99%), triethylamine (>99%), and 1,4-dioxane (>99%) were obtained from Aldrich. Diglyme was dried with molecular sieve before use. Methylene chloride was distilled over CaH_2 before use.

Telechelic hydroxylated PHB (PHB-diol) prepolymer was prepared by transesterification from the natural PHB and with diethylene glycol with dibutyltin dilaurate as a catalyst in diglyme, as previously reported (yield, 80%).[3] Purified nitrogen was used in all reactions.

Synthesis of Poly(*N*-isopropylacrylamide)-poly[(*R*)-3-hydroxybutyrate]-poly(*N*-isopropylacrylamide) Triblock Copolymers by Atom Transfer Radical Polymerization (ATRP). PHB-diol (8 g, 4.6 mmol) was dissolved in 10 mL of anhydrous methylene chloride containing 20 mmol triethylamine in a 250 mL round-bottomed flask. The reaction flask was kept in an ice/water bath (temperature = 4 °C). When the PHB-diol had completely dissolved, 10 mmol 2-bromoisobutyl bromide was added to the flask dropwise through an equalizing funnel. After addition, the reaction was allowed to proceed at room temperature for 24 h. The resulting Br-PHB-Br macroinitiator was precipitated in excess diethylether/methanol (80:20 v/v). The crude product was redissolved in tetrahydrofuran (THF) and reprecipitated in excess diethylether/methanol (80:20 v/v) to remove any residual reactants. This process was repeated another time. The yield of this reaction was ∼4.2 g (53%). The Br-PHB-Br macroinitiator for the subsequent ATRP was dried in vacuo.

The poly(*N*-isopropylacrylamide)-poly[(*R*)-3-hydroxybutyrate]-poly(*N*-isopropylacrylamide) (PNIPAAm-PHB-PNIPAAm) triblock copolymers with different PNIPAAm chain lengths were synthesized using different molar feed ratios. For example, for the synthesis of NHN(60-17-60), a molar feed ratio of [NIPAAm (6 g)]/[Br-PHB-Br (0.5 g, M_n = 1730 g/mol)]/[CuBr (84 mg)]/[HMTETA (266 mg)] of 180:1:2:4 was used. The reaction was performed in a 20 mL flask equipped with a magnetic stirrer. NIPAAm, Br-PHB-Br, and HMTETA were introduced to the flask containing 15 mL of dioxane. After the reactants had completely dissolved, the reaction mixture was degassed by bubbling nitrogen through the reaction mixture for 30 min. CuBr was added to the reaction mixture under a nitrogen atmosphere. The reaction mixture was further purged with nitrogen for 10 min. The flask was then sealed and kept under a nitrogen atmosphere. The polymerization was allowed to proceed under continuous stirring at 45 °C for 24 h. The reaction was stopped by dilution with THF and being exposed to air for 4 h. The catalyst complex was removed by passing the dilute polymer solution through a short aluminum oxide column. A colorless solution was obtained. After the removal of THF under reduced pressure, the crude copolymer was redissolved in a minimum amount of THF and precipitated in hexane to remove the unreacted NIPAAm monomer. The obtained precipitate was then dissolved in THF and then reprecipitated in diethylether. The copolymers were then dried in vacuo for further studies. The triblock copolymer yield (and the conversion of NIPAAm) after purification was 2.23 g (34.3%).

Molecular Characterization. Gel permeation chromatography (GPC) analysis was carried out with a Shimadzu SCL-10A and LC-8A system equipped with two Phenogel 5 μm 50 and 1000 Å columns (size: 300 × 4.6 mm) in series and a Shimadzu RID-10A refractive index detector. THF was used as eluent at a flow rate of 0.30 mL/min at 40 °C. Monodispersed poly(ethylene glycol) standards were used to obtain a calibration curve. The ^{1}H NMR (400 MHz) and ^{13}C NMR (100 MHz) spectra were recorded on a Bruker AV-400 NMR spectrometer at room temperature. The ^{1}H NMR measurements were carried out with an acquisition time of 3.2 s, a pulse repetition time of 2.0 s, a 30° pulse width, a 5208 Hz spectral width, and 32K data points. Chemical shift was referred to the solvent peaks (δ = 7.3 for $CHCl_3$ and 4.7 for HOD).

Critical Micelle Concentration Determination by Fluorescence Spectroscopy. Steady-state fluorescence spectra were recorded on a Shimadzu RF-5301PC spectrofluorophotometer. Excitation spectra were monitored at λ_{em} = 390 nm. Slit widths for both excitation and emission sides were maintained at 3.0 nm. Sample solutions were prepared by dissolving a predetermined amount of block copolymer in an aqueous pyrene solution of known concentration, and the solutions were allowed to stand for 1 day for equilibration. The concentration of pyrene was kept at 6.0×10^{-7} M.

Thermal Analysis. Thermogravimetric analyses (TGA) were made using a TA Instruments SDT 2960 apparatus. Samples were heated at 20 °C/min from room temperature to 800 °C under a dynamic nitrogen atmosphere (flow rate = 70 mL/min). Differential

Scheme 1. Synthesis of PNIPAAm-PHB-PNIPAAm Triblock Copolymers by ATRP

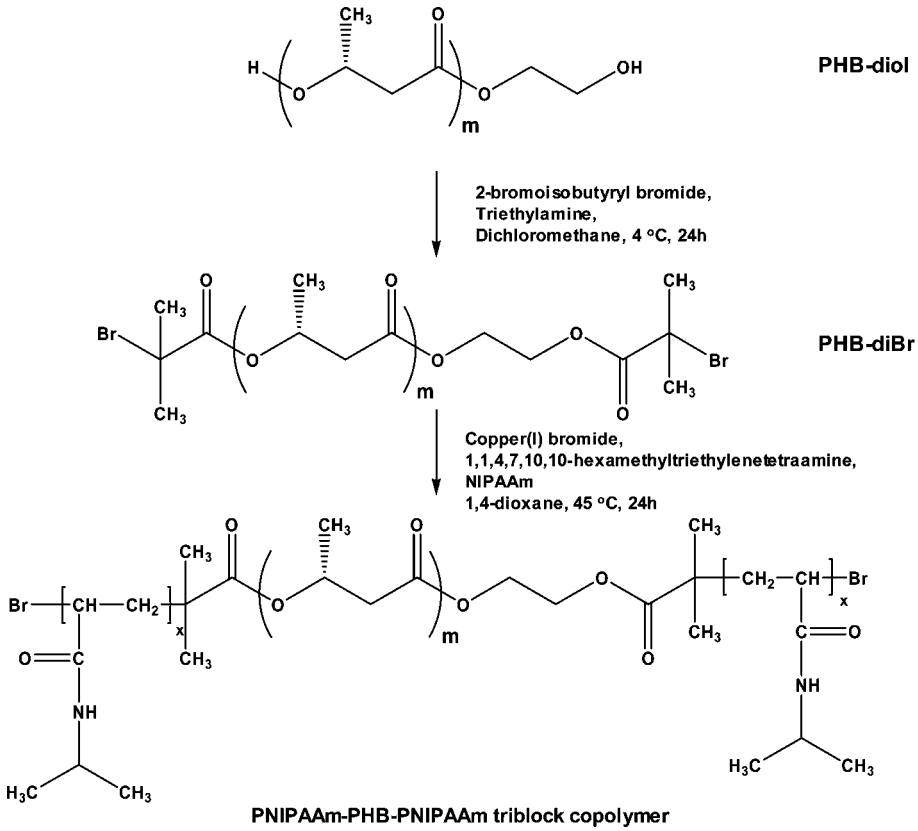

scanning calorimetry (DSC) measurements were performed using a TA Instruments 2920 differential scanning calorimeter equipped with an autocool accessory and calibrated using indium. The following protocol was used for each sample: heating from room temperature to 170 at 20 °C/min, holding at 170 °C for 2 min, cooling from 170 to −30 at 5 °C/min, and reheating from −30 to 170 at 5 °C/min. Data were collected during the second heating run. Transition temperatures were taken as peak maxima.

Lower Critical Solution Temperature Determination. Cloud points were measured with a UV−vis spectrophotometer. Aqueous copolymer solutions (0.5 mg/mL) were heated at 2 °C/min while both the transmittance at 500 nm (1 cm path length) and the solution temperature were monitored.

Micelle Size Measurements. Measurements of micelle size were performed on micelle solutions (50 mg/L) using a Zetasizer Nano ZS (Malvern Instruments, Southborough, MA) with a laser light wavelength of 633 nm at a 173° scattering angle. The micelle size measurement was performed at 25 °C. The deconvolution of the measured correlation curve to an intensity size distribution was accomplished using a nonnegative least-squares algorithm. The decay rate distributions were transformed to an apparent diffusion coefficient (D). From the diffusion coefficient, the apparent hydrodynamic size of the polymer or micelles can be obtained by the Stokes−Einstein equation. The Z-average hydrodynamic diameters of the particles were given by the instrument. The Z-average size is the intensity-weighted mean diameter derived from a cumulant or single-exponential fit of the intensity autocorrelation function.

Transmission Electron Microscopy. The samples were imaged on a JEOL JEM-2010F FasTEM field emission transmission electron microscope operated at 100 kV. We prepared the samples for TEM by directly depositing one drop of sample solution (50 or 500 mg/L) containing 0.1 wt % phosphotungstic acid (PTA) onto copper grids, which were coated in advance with supportive Formvar films and carbon (Agar Scientific). The samples were kept in an oven for 12 h for drying at 25 or 35 °C before TEM imaging.

Cells and Media. L929 mouse fibroblasts were obtained from ATCC and cultivated in DMEM containing 10% fetal bovine serum (FBS) and 1% penicillin/streptomycin. Cells were grown as a monolayer and were passaged upon confluence using trypsin (0.5% w/v in PBS). L929 cells were harvested from culture by incubating in trypsin solution for 10 min. The cells were centrifuged and the supernatant was discarded. Three mL of serum-supplemented DMEM was added to neutralize any residual trypsin. The cells were resuspended in serum-supplemented DMEM at a concentration of 2×10^4 cells mL^{-1}. Cells were cultivated at 37 °C and 5% CO_2.

Cell Viability Assay. The cytotoxicity of the copolymers was evaluated using the MTT assay in L929 cell lines. The cells were cultured in complete DMEM supplemented with 10% FBS at 37 °C, 5% CO_2, and 95% relative humidity. The cells were seeded in a 96-well microtiter plate (Nunc, Wiesbaden, Germany) at densities of 3×10^4 cells/well. After 24 h, culture media were replaced with serum-supplemented culture media containing known concentrations of the copolymers, and the cells were incubated for a further 48 h. Then, 10 μL of sterile-filtered MTT stock solution in PBS (5 mg/mL) was added to each well, reaching a final MTT concentration of 0.5 mg/mL. After 5 h, unreacted dye was removed by aspiration. The formazan crystals were dissolved in DMSO (100 μL/well), and the absorbance was measured using a microplate reader (Spectra Plus, TECAN) at a wavelength of 570 nm. The relative cell viability (%) related to control cells cultured in media without polymers was calculated with $[A]_{test}/[A]_{control} \times 100\%$, where $[A]_{test}$ is the absorbance of the wells with polymers and $[A]_{control}$ is the absorbance of the control wells. All experiments were conducted with six repetitions and averaged.

Results and Discussion

Synthesis of the PNIPAAm-PHB-PNIPAAm Triblock Copolymers via Atom Transfer Radical Polymerization. The thermo-responsive PNIPAAm-PHB-PNIPAAm triblock copolymers were prepared according to the reaction sequence shown in Scheme 1. The starting dibromo-terminated PHB (Br-PHB-

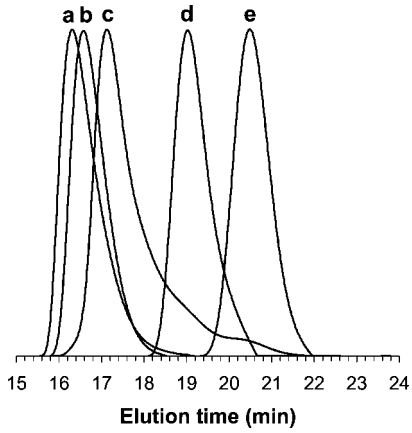

Figure 1. GPC traces of the PNIPAAm-PHB-PNIPAAm triblock copolymers and the PHB precursor: (a) NHN(180-17-180), (b) NHN(157-17-157), (c) NHN(60-17-60), (d) NHN(10-17-10), and (e) PHB-diBr.

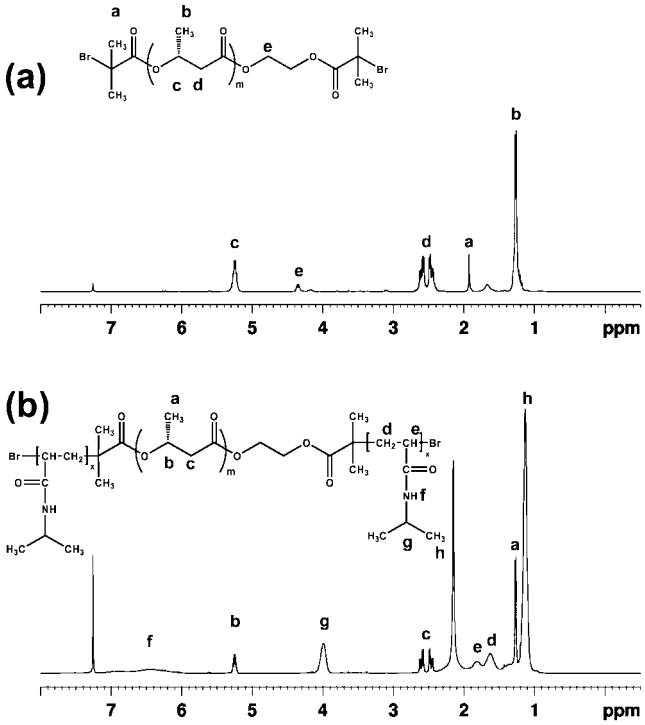

Figure 2. ^{1}H NMR spectrum of (a) PHB-diBr and (b) PNIPAAm-PHB-PNIPAAm triblock copolymer, NHN(10-17-10).

Br) macroinitiator for ATRP was prepared from PHB-diol by the reaction of the terminal hydroxyl end groups of PHB-diol with 2-bromoisobutyryl bromide. The M_n of Br-PHB-Br is $\sim 1.73 \times 10^3$ g/mol (Figure 1e). The ^{1}H NMR spectrum shows a signal at 4.25 ppm because of the protons from the ethylene glycol segment in the PHB-diBr and a signal at 1.92 ppm from the methyl protons of the 2-bromoisobutyryl fragment (Figure 2a). By calculating the ratio of these two signals, we obtained the extent of substitution of the PHB-diol. Substitution of the hydroxyl groups was estimated to be ~95% on the basis of ^{1}H NMR. PNIPAAm-PHB-PNIPAAm triblock copolymer was synthesized via ATRP of NIPAAm from the Br-PHB-Br macroinitiator. The PNIPAAm-PHB-PNIPAAm triblock copolymers were synthesized in dioxane at 45 °C for 24 h via ATRP of NIPAAm from the Br-PHB-Br macroinitiator units. A series of triblock copolymers with different PNIPAAm block length were synthesized by varying the monomer feed. The molecular weights of the copolymers are summarized in Table 1. In general, the copolymers had low polydispersities, and the GPC profiles of the copolymers did not show overlapping peaks with the PHB-diBr precursor, as shown in Figure 1. This indicates that the PHB-diBr has reacted with the NIPAAm monomer.

The chemical structure of the PNIPAAm-PHB-PNIPAAm triblock copolymer was characterized by ^{1}H NMR spectroscopy. Figure 2b shows the ^{1}H NMR spectrum of the NHN(10-17-10) copolymer. The peaks associated with the methyl protons (δ = 1.14), methylene protons (δ = 1.4 to 1.6), methylidyne protons adjacent to the carbonyl group (δ = 1.78), and methylidyne protons adjacent to the amine moiety (δ = 3.95) of the PNIPAAm blocks were observed. The peaks associated with the methyl proton (δ = 1.32), methylene proton (δ = 2.49 to 2.64), and methine proton (δ = 5.25) of the PHB segment were also observed. From ^{1}H NMR, the molecular weights and composition of the block copolymers were calculated and are summarized in Table 1. For ^{13}C NMR, the spectrum of NHN(10-17-10) copolymer is shown in Figure 3. The peaks associated with the methyl carbons (δ = 22.3), methylene carbons and methylidyne carbon adjacent to the carbonyl group (δ = 33.4−38.2), methylidyne carbon adjacent to the amine moiety (δ = 40.1), and carbonyl carbon (δ = 175.2) of the PNIPAAm blocks were observed. The peaks associated with the methyl carbon (δ = 19.9), methylene carbon (δ = 41.2), methine carbon (δ = 68.1), and carbonyl carbon (δ = 170.1) of the PHB segment were observed. More importantly, the methyl carbon peak associated with the 2-bromoisobutyryl fragment, originally at δ = 31.0, was absent; this indicates that the bromide end of the macroinitiator has reacted with the NIPAAm monomer. Therefore, the NMR results taken together with the GPC results demonstrate the successful synthesis of the triblock copolymers.

Core−Shell Micelle Formation. NMR spectroscopy was used to investigate the effect of solvent on the micelle structure.[36−39] $CDCl_3$ is a good nonselective solvent for PHB and PNIPAAm, where water is a good selective solvent for PNIPAAm but is poor for PHB. In $CDCl_3$, the peaks due to the PHB and PNIPAAm segments were sharp and well-defined. (See the Supporting Information, Figures S1 and S2.) In D_2O, PNIPAAm is shown as a sharp peak, but PHB peaks could not be observed. This shows that the molecular motion of PHB is slow in water, which indicates a hydrophobic core structure made up of PHB with the hydrophilic PNIPAAm as the outer corona structure, confirming the core−corona structure of the micelle.[37−39]

Critical Micelle Concentration Determination. The PNIPAAm-PHB-PNIPAAm triblock copolymers were soluble in water. CMC determination was carried out for these copolymers by the use of fluorescence spectroscopy. The fluorescence probe technique is a powerful tool for studying micellar properties of amphiphilic block copolymers.[40,41] When the copolymer concentration in an aqueous solution of pyrene is increased, both emission and excitation spectra undergo significant changes upon micellization of the block copolymer systems.[41] These changes are caused by the transfer of pyrene molecules from the polar aqueous environment to the hydrophobic micellar cores and are related to the location of the pyrene molecules in the solution. The fluorescence excitation spectrum shows a shift in the low-energy band of the L_a ($S_2 \leftarrow S_0$) from 333 to 338 nm. It has been reported that this (0,0) absorption band change of pyrene is more sensitive to the true onset of aggregation than to either lifetime measurements or fluorescence emission changes.[42,43] This change is described in terms of the ratio of the intensities of the first and third bands in the pyrene fluorescence spectrum, I_{338}/I_{333}. Hence, the CMC values of the PNIPAAm-PHB-PNIPAAm triblock copolymers

Table 1. Molecular Characteristics of PNIPAAm-PHB-PNIPAAm Triblock Copolymers

copolymer[a]	M_n ($\times 10^3$)[b]	M_w/M_n[b]	M_n ($\times 10^3$)[c]	copolymer composition (wt %)[c] PHB	copolymer composition (wt %)[c] NIPAAm	copolymer composition (wt %)[d] PHB	copolymer composition (wt %)[d] NIPAAm
PHB-diBr	1.73	1.04	1.63				
NHN(10-17-10)	3.75	1.09	2.79	58.5	41.5	59.5	40.5
NHN(60-17-60)	13.76	1.49	8.23	19.8	80.2	23.8	76.2
NHN(157-17-157)	33.20	1.30	31.35	5.2	94.8	6.3	93.7
NHN(180-17-180)	37.72	1.50	41.80	3.9	96.1	3.5	96.5

[a] PNIPAAm-PHB-PNIPAAm triblock copolymers are denoted NHN (N for PNIPAAm and H for PHB). The numbers in brackets show the indicative molecular weight of the respective block in hundreds of grams per mole. [b] Determined by GPC. [c] Calculated from ^{1}H NMR results. [d] Calculated from TGA results.

Table 2. Solution Properties of PNIPAAm-PHB-PNIPAAm Triblock Copolymers

copolymer	LCST (°C)[a]	CMC (mg/L)[b]	K_v ($\times 10^{-5}$)	d, 25 °C (nm)[c]	d, 35 °C (nm)[c]
NHN(10-17-10)	28.0	1.5	20.42	844 ± 24 (0.97)	550 ± 18 (0.47)
NHN(60-17-60)	28.3	10.8	2.71	449 ± 27 (0.77)	215 ± 2 (0.30)
NHN(157-17-157)	28.8	38.1	2.33	342 ± 39 (0.48)	161 ± 2 (0.15)
NHN(180-17-180)	29.0	41.1	1.64	287 ± 22 (0.45)	139 ± 3 (0.14)

[a] Determined from turbidmetry measurements. [b] Determined by pyrene solubilization method. [c] Mean Z-average diameters by dynamic light scattering from five individual measurements. Numbers in brackets represent the average polydispersity of the particle size.

Table 3. Transition Temperatures, Corresponding Enthalpies, Crystallinity for Polymer Samples, and Their Decomposition Temperatures

copolymer	T_m (°C)[a]	ΔH_m (J/g)[b]	X_c (%)[c]	T_d, PHB (°C)[d]	T_d, PNIPAAm (°C)[d]
PHB-diBr	142.2	62.5	42.6	235.9	
NHN(10-17-10)	137.3	53.8	36.7	244.9	361.1
NHN(60-17-60)	135.6	32.8	22.4	284.6	364.5
NHN(157-17-157)	129.5	23.2	15.8	291.4	366.1
NHN(180-17-180)	124.3	10.7	7.3	291.9	367.4

[a] Melting point determined by DSC second heating run. For PHB-diBr having multipeak endotherm because of melting recrystallization, the T_m value for the second peak is given. [b] Enthalpy change during melting determined by DSC second heating run. $\Delta H_m = \Delta H_i/w_i$, where ΔH_i is the area of the endothermic peak for PHB block read from Figure 9, and w_i is the weight fraction of the corresponding block. [c] Crystallinity calculated from melting enthalpies. Reference values of 146.6 J/g for completely crystallized PHB were used.[3] [d] Temperature at which the onset of thermal degradation occurred.

in aqueous solution were determined using the fluorescence excitation spectra of the pyrene probe.

Figure 4a shows the excitation spectra for pyrene in water at various concentrations of PNIPAAm-PHB-PNIPAAm triblock copolymer. When the copolymer concentration increased, a red shift in the (0,0) absorption band from 333 to 338 nm was observed. Figure 4b shows the intensity ratio of I_{338}/I_{333} of pyrene excitation spectra as a function of the logarithm of copolymer concentrations for NHN(60-17-60) triblock copolymer. The I_{338}/I_{333} versus log C plots present a sigmoid curve. A negligible change in the intensity ratio of I_{338}/I_{333} was observed in the low concentration range for each triblock copolymer. With an increase in the copolymer concentration, the intensity ratio exhibited a substantial increase at a certain concentration, reflecting the incorporation of pyrene into the hydrophobic core region of the micelles. Therefore, the CMC values were determined form the cross-over point in the low concentration range in Figure 4b, and the results are listed in Table 2. The very low CMC values for PNIPAAm-PHB-PNIPAAm triblock copolymers indicate a very strong tendency of the triblock copolymers toward the formation of micelles in aqueous solution. The CMC values of the triblock copolymers were observed to increase with an increase in the PNIPAAm segment length because of the increased hydrophilicity of the copolymer. The CMC values of the PNIPAAm-PHB-PNIPAAm triblock copolymers are much lower than those of the PNIPAAm-PCL-PNIPAAm[30] and PCL-PNIPAAm-PCL[31] copolymers, indicating that the more hydrophobic PHB segments (as compared with PCL) provide a greater driving force for the self-assembly of the copolymers into micelles in aqueous solution.

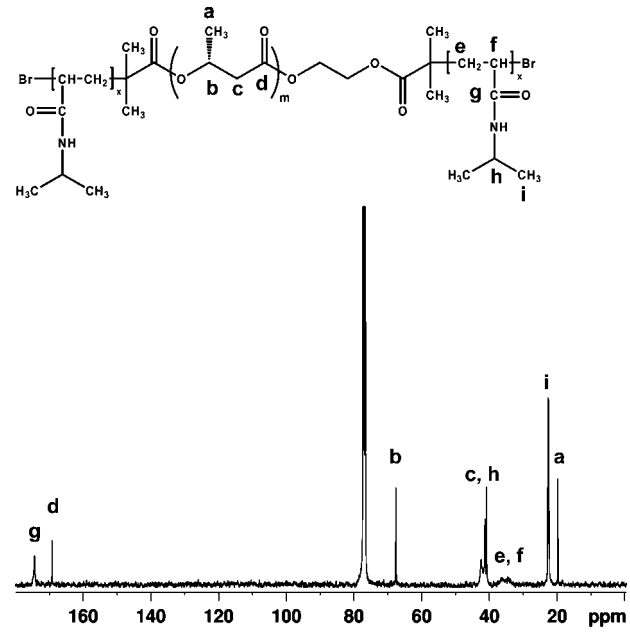

Figure 3. ^{13}C NMR spectrum of PNIPAAm-PHB-PNIPAAm triblock copolymer, NHN(10-17-10).

Partitioning of Pyrene in Micelles. These micelles can aid in the encapsulation and aqueous solubilization of hydrophobic drugs. The encapsulation efficiency of the drug is affected by the hydrophobicity of the micelle core. The hydrophobicity of the PHB micellar core can be estimated by determining the partition equilibrium coefficient, K_v of pyrene in the aqueous PNIPAAm-PHB-PNIPAAm triblock copolymer solutions. The calculations were performed as previously reported.[41,44−46] This method calculates the partition equilibrium on the basis of the assumption of a simple equilibrium distribution between the micellar phase and the water phase. The ratio of the pyrene concentration in the micellar phase to the water phase ($[Py]_m/[Py]_w$) can be correlated to the ratio of volume of each phase and is expressed as follows

$$([Py]_m/[Py]_w) = K_v V_m/V_w \quad (1)$$

This can be rewritten as

$$([Py]_m/[Py]_w) = K_v x(c - \mathrm{CMC})/1000\rho \quad (2)$$

where x is the weight fraction of the PHB block in the triblock copolymer, c is the concentration of the triblock copolymer,

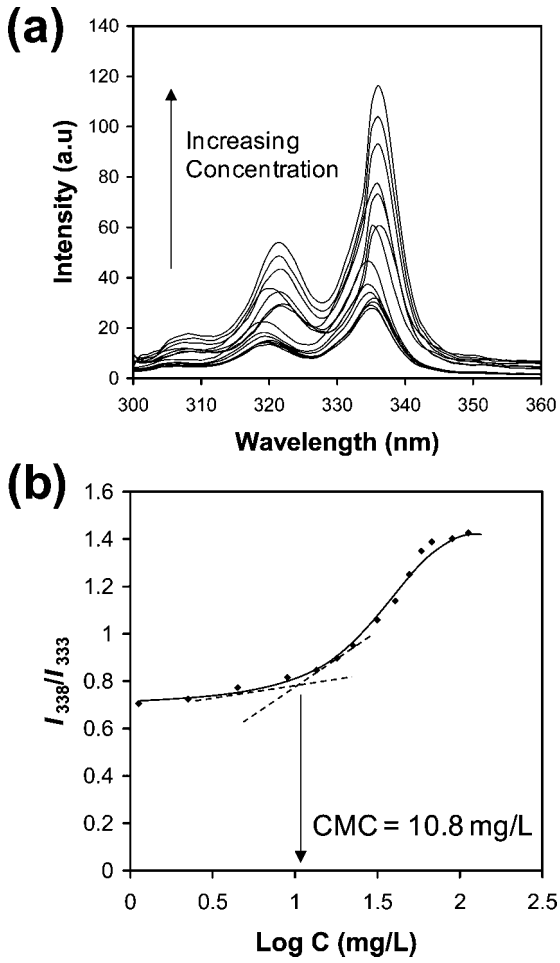

Figure 4. (a) Steady-state fluorescence excitation spectra monitored at 390 nm for the pyrene probe in an aqueous solution of NHN(60-17-60) copolymer of various concentrations in water at 25 °C. The concentration of pyrene is 6.0×10^{-7} M. (b) Plots of the I_{338}/I_{333} ratio of pyrene excitation spectra in water as a function of NHN(60-17-60) triblock copolymer concentration at 25 °C.

and ρ is the density of the PHB core of the micelles, which is assumed to be the bulk density of PHB (1.285 g/cm^3). In the intermediate range of the polymer concentration with substantial increases in the intensity ratios (I_{338}/I_{333}), $([Py]_m/[Py]_w)$ can be written as

$$([Py]_m/[Py]_w) = (F - F_{min})/(F_{max} - F) \quad (3)$$

where F_{min} and F_{max} correspond to the average magnitude of the intensity ratio (I_{338}/I_{333}) in the constant region in the low and high concentration ranges in Figure 4, respectively. F is the intensity ratio (I_{338}/I_{333}) in the intermediate concentration range of the triblock copolymers. Combining eqs 2 and 3 yields

$$(F - F_{min})/(F_{max} - F) = K_v x(c - \mathrm{CMC})/1000\rho \quad (4)$$

We obtained K_v values for pyrene were obtained by plotting a graph of $(F - F_{min})/(F_{max} - F)$ versus the concentration of the PNIPAAm-PHB-PNIPAAm triblock copolymer solutions. (See the Supporting Information, Figure S3.) The K_v values are summarized in Table 2. The values ranged from (1.64−20.42) $\times 10^5$ for the triblock copolymers. This indicates that the copolymer can be potentially loaded with a hydrophobic drug with high encapsulation efficiency. As the length of the PNIPAAm chains increased, the K_v values decreased, suggesting that the hydrophobicities of the micellar core decreased. This is related to the hydrophilic/hydrophobic balance in the triblock copolymer, which consequently affects the micelle packing

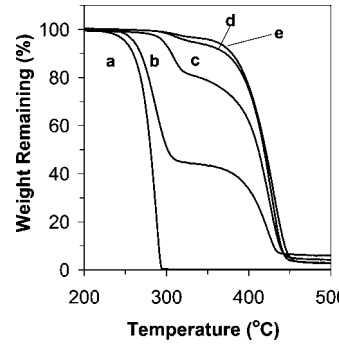

Figure 5. TGA curves obtained at a heating rate of 20°C/min under a nitrogen atmosphere for (a) PHB-diBr, (b) NHN(10-17-10), (c) NHN(60-17-60), (d) NHN(157-17-157), and (e) NHN(180-17-180).

ability of the copolymer. Previously, K_v values of 3.0×10^4 to 3.3×10^5 have been reported for amphiphilic poly[bis(2,2,2-trifluoroethoxy)phosphazene]/poly(propylene glycol) triblock copolymers, and K_v values of $(1.79-5.88) \times 10^5$ have been reported for copolymers of poly(2-ethyl-2-oxazoline)-poly(ε-caprolactone) and poly(2-ethyl-2-oxazoline)-poly(L-lactide).[45,46] The K_v values determined in this work are relatively higher than those previously reported, particularly for NHN(10-17-10). Compared with the K_v values of PNIPAAm-PCL-PNIPAAm micelles, the K_v values of PNIPAAm-PHB-PNIPAAm are much higher.[30] It appears that PNIPAAm-PHB-PNIPAAm micelles have a higher encapsulation capacity than do PNIPAAm-PCL-PNIPAAm micelles.

Thermal Stability. The thermal stability of the triblock copolymers was evaluated using thermogravimetric analysis (TGA). Figure 5 shows the weight-loss curves for the series of triblock copolymers compared with its PHB precursor. The PNIPAAm-PHB-PNIPAAm triblock copolymers undergo stepwise thermal degradation. The PHB block degrades first at ~230 °C, followed by the PNIPAAm block at ~360 °C. The PNIPAAm block starts to degrade only after the PHB block has completed its degradation at 310−330 °C. The compositions of the triblock copolymers can be calculated from the two-step degradation profile. The PHB and PNIPAAm contents estimated from TGA results are listed in Table 1. The results are in excellent agreement with the values calculated from ^{1}H NMR. We evaluated the thermal stabilities of these polymers by observing the temperature at which the onset of thermal degradation occurs. The thermal stability of PHB increased when it was incorporated in the triblock copolymers as compared with the PHB-diBr precursor. Overall, the copolymers have better thermal stabilities than their PHB precursors.

Solid-State Behavior. DSC was carried out to determine the microphase separation and crystallization of the PHB block in the copolymer. The DSC thermograms for the PNIPAAm-PHB-PNIPAAm triblock copolymers are presented (Supporting Information, Figure S4). Numerical values corresponding to the thermal transitions and the crystallinity of the PHB block are tabulated in Table 2. PHB is a crystalline polymer. With the incorporation of PNIPAAm, the crystallization of the PHB block is suppressed. When the length of the PNIPAAm block increased, the fractional crystallinity of the PHB block decreased. The melting transition corresponding to PHB segments shifted to a lower temperature with a lower crystallinity in comparison with that of their PHB-diBr precursors. The decreases in T_m and crystallinity are determined by the relative fractions of PHB segments in the copolymers. For example, the T_m and crystallinity of the PHB segment decrease from 137.3 °C and 36.7% for NHN(10-17-10) to 124.3 °C and 10.7% for NHN(180-17-180), respectively. When the copolymers are cooled from the molten state, the PHB segment solidifies and crystallizes

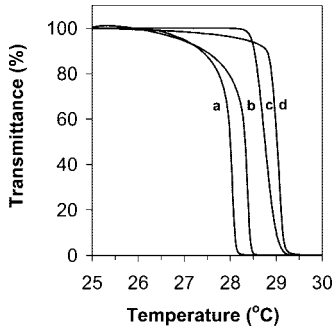

Figure 6. Thermoresponsive behavior of PNIPAAm-PHB-PNIPAAm micelles (0.5 mg/mL) (a) NHN(10-17-10), (b) NHN(60-17-60), (c) NHN(157-17-157), and (d) NHN(180-17-180).

However, because of the interference of the PNIPAAm segment, the crystallization of the PHB segment is retarded.

Thermoresponsive Behavior of Micelles. The PNIPAAm-PHB-PNIPAAm triblock copolymer micelles were water-soluble at 25 °C with a hydrophobic PHB core and hydrophillic PNIPAAm corona. When the temperature of the solution is increased, the hydrophobicity of PNIPAAm increases and PNIPAAm chains in the micelle corona collapse. The increased hydrophobicity of the micelles leads to micelle aggregation, which leads to the formation of larger particles. We demonstrated the thermosensitivity of the PNIPAAm-PHB-PNIPAAm triblock copolymer micelles by observing the change in the optical absorbance of a micellar solution as a function of temperature. PNIPAAm exhibits a temperature-sensitive phase transition in the temperature range of 32 to 33 °C. This temperature is known as the LCST. The LCST values of the copolymers are presented in Table 2. At temperatures below LCST, PNIPAAm is a hydrophilic water-soluble polymer. Above this temperature, PNIPAAm becomes hydrophobic and precipitates out of the aqueous solution. In this article, the LCST is defined as the temperature exhibiting a 50% decrease in optical transmittance of an aqueous copolymer solution (0.5 mg/mL) at 500 nm (Figure 6). The incorporation of the hydrophobic PHB lowers the LCST compared with the PNIPAAm homopolymer. The copolymer NHN(10-17-10) exhibits an LCST of 28.0 °C, whereas the copolymer NHN(180-17-180) shows an LCST of 29.0 °C. In this work, the LCST values of the copolymers are expected to increase to a constant value with increasing PNIPAAm chain length. The changes observed in this case are due to the changes in the polymer/solvent interactions arising from the change in the hydrophillic/hydrophobic balance of the copolymers. For the PNIPAAm-PHB-PNIPAAm triblock copolymers, the copolymers become more hydrophilic as the PNIPAAm segments become longer, leading to the observed increase in the LCST. Overall, there is no significant change in the LCST values with the incorporation of the hydrophobic PHB segment. This is similar to previously reported studies on PNIPAAm-PCL-PNIPAAm and PCL-PNIPAAm-PCL copolymer micelles.[30,31] From this, we hypothesize that the thermosensitive PNIPAAm arms of the micelle behave like free PNIPAAm in solution, except that they are anchored in a micelle structure by the hydrophobic PHB segments. PCL-PNIPAAm-PCL copolymer micelles showed no decrease in the LCST values upon incorporation of PCL in the copolymer. The authors suggested that the copolymers form phase-separated core−shell micelle structures in aqueous solution.[31]

The phenomenon of LCST is a complex process that is dependent on the concentration of the copolymer solution.[47] Thermoresponsive behavior of PNIPAAm, such as the coil-to-globule transition, was reported using dilute solutions.[48,49] Therefore, for our study of the thermoresponsive behavior of the micelles, we used very dilute solutions that were just slightly above the CMC value. The scheme of the thermoresponsive micelle behavior of these copolymers in a dilute solution is illustrated in Figure 7a. The morphology and size distributions of the copolymer micelles were investigated by TEM observation (Figure 7b) and dynamic light scattering (DLS) (Figure 7c), respectively. The schematic relation between the proposed structure of the micelle aggregates and the TEM-observed structure is shown in Figure 7d. The results of the DLS measurements are summarized in Table 2. From DLS measurements, these diameters of the micelles range from 290 to 840 nm, decreasing as the PNIPAAm segment becomes longer. This is an interesting observation. Normally, we would expect that with a longer PNIPAAM chain, the micelle size would increase with increasing micelle interaction with water. However, in this case, the reverse trend is observed. We attribute this to micelle aggregation. PHB is a very hydrophobic copolymer that has a very strong tendency to self-associate.[42] For the copolymers with higher PHB content, there is a great tendency for the PHB segments to associate in the aqueous environment. This observation corroborates with the partition coefficient of pyrene that was calculated in the earlier section, which showed that the PHB core is very hydrophobic. It is also pertinent that in this experiment, the samples were not filtered prior to measurements so that the pristine state of the dissolved copolymer could be analyzed. The contour length of NHN(180-17-180) is calculated to be ∼100 nm, with the PHB segment estimated to be ∼8 nm and the PNIPAAm segment estimated to be ∼96 nm. However, the observed particle size in the DLS experiment is 290 nm. Therefore, in this experiment, it is very likely that micelle aggregates are observed. When the temperature is increased to 35 °C, the particle size decreases because of the collapse of the PNIPAAm corona and increased hydrophobic interactions between the PHB cores, leading to an overall decrease in the aggregate size (Figure 7a). The diameters of the micelles range from 140 to 550 nm. Lower polydispersities were observed at this temperature. We should note that the initial PHB segment used is almost monodisperse in terms of molecular weight. This observation is most likely caused by the collapse of the PNIPAAm corona in the PHB core. The particle size remained constant at this temperature for at least 24 h and did not form aggregates. The solutions were observed to be transparent and very faint blue. The micelles of this size are not expected to be readily cleared by renal filtration, as inferred by previous in vivo studies.[33−35] The pore size of the glomerular basement membrane is ∼3−5 nm, which is too small for the micelles to pass.[35] This allows for the prolonged circulation of the drug-loaded micelles in the system. After the drug cargo is released, the micelles will hydrolytically degrade. Upon complete degradation of the copolymer, we expect only the monomers of D-3-hydroxybutyric acid and the undegraded PNIPAAm segments (molecular weight <20 000 g/mol) to be left. These fragments can be easily removed by renal filtration.[33−35] The TEM micrographs of NHN(180-17-180) copolymer solution (50 mg/L) dried at 25 and 35 °C are shown in Figure 8. The results support the observations made with DLS. Larger spherical particles (ca. 200 nm) were observed for the sample dried at 25 °C, whereas smaller particles (ca. 100 nm) were observed for the sample dried at 35 °C. In addition, it was observed that upon drying at 35 °C, the micelle aggregates were packed more densely, although large micron-sized particles were not observed. This is probably due to the low concentration of the solution.

The concentration effect on the aggregation behavior was further evaluated. LCST behavior has been reported to be dependent on the concentration of the solution.[47] When the

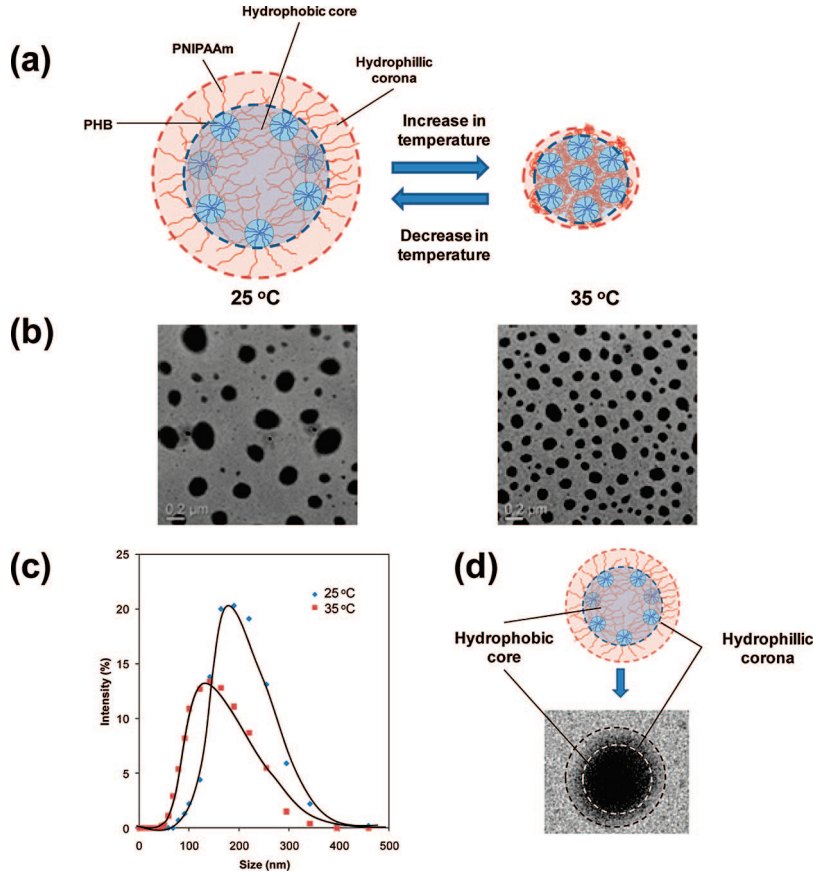

Figure 7. (a) Proposed thermoresponsive behavior of PNIPAAm-PHB-PNIPAAm triblock copolymers. (b) TEM micrographs of the NHN(180-17-180) micelles prepared at 25 and 35 °C. (c) Particle size distribution of NHN(180-17-180) micelles (solution concentration = 50 mg/L) at 25 and 35 °C. (d) Schematic relation between the proposed structure of the micelle aggregates and the TEM-observed structure.

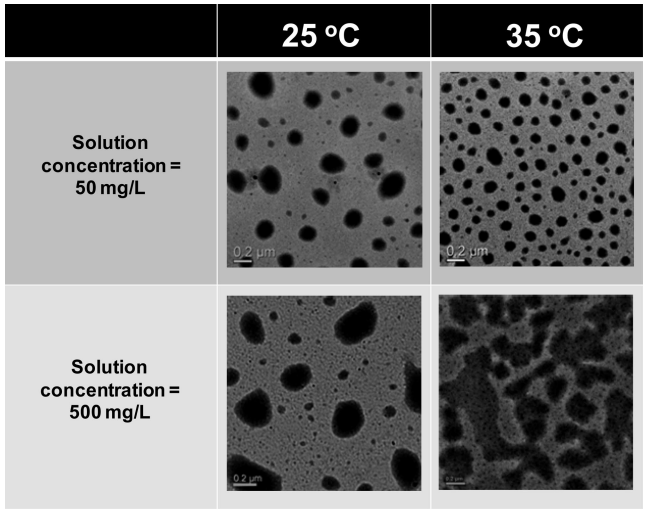

Figure 8. TEM micrographs of the NHN(180-17-180) micelles prepared at 25 and 35 °C at 50 and 500 mg/L.

concentration of the solution is high, there is a great decrease in the optical transmittance of the solution. However, when the concentration of the solution is low, the change in the optical transmitrance of the solution is not so obvious. For example, Fujishige[48] and Hirotsu[49] have reported the collapse of PNIPAAm chains at very dilute polymer concentrations on the basis of light scattering experiments. At very low concentrations, no PNIPAAm aggregation is observed. TEM micrographs of NHN(180-17-180) copolymer solutions (50 and 500 mg/L) dried at 25 and 35 °C are shown in Figure 8. Comparing both solutions at 25 °C, the 500 mg/L solution had slightly larger aggregates.

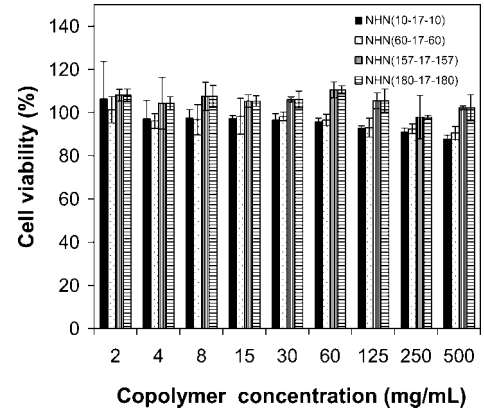

Figure 9. Cell viability of L929 cells incubated with known concentrations of PNIPAAm-PHB-PNIPAAm triblock copolymers.

Above the solution LCST, at 35 °C, the behavior is very different. Whereas smaller dense particles were observed for the sample prepared at 50 mg/L and dried at 35 °C, large patchy aggregates were observed for the sample prepared from the 500 mg/L solution and dried at 35 °C. When the concentration is sufficiently high, the increased temperature leads to the typical LCST behavior. This was demonstrated by the turbidity experiments described earlier. Large irregular aggregates with sizes of >1 μm are observed. This is similar to another report in which PDLLA-PNIPAAm diblock copolymers were observed to undergo aggregation at temperatures above the LCST.[32]

Cytotoxicity Study. We evaluated the cytotoxicity of the triblock copolymers by incubating the mouse fibroblast L929 cells with different concentrations of the copolymer solution

over a period of 48 h at 37 °C. The aim of this experiment is to determine the potential toxicological hazard of the copolymers. Quantification of the cytotoxic response was performed using the MTT assay, as shown in Figure 9. The copolymer solutions do not show significant cytotoxicity against L929 cells over a solution concentration range of 2−500 mg/mL. Interestingly, we noticed that the cell viability increased with increasing PNIPAAm content in the block copolymer. From the MTT assay results of the copolymers, we expect the polymer to be safe for biomedical applications.

Conclusions

Thermoresponsive triblock copolymers that have two hydrophilic PNIPAAm blocks linked to a central hydrophobic PHB block were synthesized by ATRP. Molecular characterizations of the copolymers were performed by GPC, NMR, TGA, and DSC. The triblock copolymers formed micelles with a hydrophobic PHB core and a hydrophilic PNIPAAm shell, as inferred from the ^{1}H and ^{13}C NMR spectra derived in two different environments ($CDCl_3$ and D_2O). The CMCs of the triblock copolymers were very low and have great stability under high dilution conditions. We estimated the hydrophobicity of the micellar cores by measuring the partition equilibrium constant, K_v, of pyrene in the micellar solution of the triblock copolymers. The high values of K_v indicate the potential high encapsulation efficiency of hydrophobic drugs. The hydrophobicity of the micellar core could be controlled by adjusting the composition of the copolymer. The temperature sensitivity of the triblock copolymer micelles was studied by the turbimetry method. A preliminary cytotoxicity evaluation of the copolymers indicates that these copolymers are nontoxic. The exciting potential for this copolymer lies in its low critical micelle concentrations, the tunability of these loading capacities by variation in its composition, and its potential biodegradability.

Acknowledgment. The authors acknowledge the financial support from National University of Singapore and Institute of Materials Research and Engineering, A*STAR, Singapore. The authors thank M.J. Loh and J.G. Lim for kindly proofreading the manuscript. X.J. Loh would like to acknowledge the A*STAR Graduate Scholarship.

Supporting Information Available: ^{1}H NMR and ^{13}C NMR spectra of of NHN(10-17-10), plots of $(F - F_{min})/(F_{max} - F)$ versus concentration of PNIPAAm-PHB-PNIPAAm triblock copolymers, and DSC second heating curves. This material is available free of charge via the Internet at http://pubs.acs.org.

References and Notes

(1) Torchilin, V. P. *J. Controlled Release* **2001**, *73*, 137–172.
(2) Kwon, G. S.; Kataoka, K. *Adv. Drug Delivery Rev.* **1995**, *16*, 295–309.
(3) Li, J.; Li, X.; Ni, X.; Leong, K. W. *Macromolecules* **2003**, *36*, 2661–2667.
(4) Paria, S. *Adv. Colloid Interface Sci.* **2008**, *131*, 24–58.
(5) Walker, L. M.; Kuntz, D. M. *Curr. Opin. Colloid Interface Sci.* **2007**, *12*, 101–105.
(6) Wang, Z. L. *Appl. Microbiol. Biotechnol.* **2007**, *75*, 1–10.
(7) Fiamegos, Y. C.; Stalikas, C. D. *Anal. Chim. Acta* **2005**, *550*, 1–12.
(8) *Biopolymers, Polyesters I-III*; Doi, Y.; Steinbuchel, A., Eds.; Wiley: New York, 2001; Vols. 3, 3b, and 4.
(9) Doi, Y. *Microbial Polyesters*; VCH: New York, 1990.
(10) Anderson, A. J.; Dawes, E. A. *Microbiol. Rev.* **1990**, *54*, 450–472.
(11) *Novel Biodegradable Microbial Polymers*; Dawes, E. A., Ed.; Kluwer: Dordrecht, The Netherlands, 1990.
(12) Satkowski, M. M.; Melik, D. H.; Autran, J. P.; Green, P. R.; Noda, I.; Schechtman, L. A. In *Biopolymers*; Steinbuchel, A.; Doi, Y., Eds.; Wiley-VCH: Wienheim, Germany, 2001; p 231.
(13) Iwata, T.; Doi, Y. *Macromol. Chem. Phys.* **1999**, *200*, 2429–2442.
(14) Purnell, M. P.; Petrasovits, L. A.; Nielsen, L. K.; Brumbley, S. M. *Plant Biotechnol. J.* **2007**, *5*, 173–184.
(15) Reusch, R. N. *Can. J. Microbiol.* **1995**, *41*, 50–54.
(16) Loh, X. J.; Goh, S. H.; Li, J. *Biomacromolecules* **2007**, *8*, 585–593.
(17) Loh, X. J.; Goh, S. H.; Li, J. *Biomaterials* **2007**, *28*, 4113–4123.
(18) Loh, X. J.; Li, J. *Expert Opin. Ther. Pat.* **2007**, *17*, 965–977.
(19) Motokawa, R.; Morishita, K.; Koizumi, S.; Nakahira, T.; Annaka, M. *Macromolecules* **2005**, *38*, 5748–5760.
(20) Kim, Y. C.; Kil, D. S.; Kim, J. C. *J. Appl. Polym. Sci.* **2006**, *101*, 1833–1841.
(21) Wei, H.; Zhang, X. Z.; Cheng, C.; Cheng, S. X.; Zhuo, R. X. *Biomaterials* **2007**, *28*, 99–107.
(22) Li, Y. Y.; Zhang, X. Z.; Cheng, H.; Kim, G. C.; Cheng, S. X.; Zhuo, R. X. *Biomacromolecules* **2006**, *7*, 2956–2960.
(23) Wei, H.; Zhang, X. Z.; Cheng, H.; Chen, W. Q.; Cheng, S. X.; Zhuo, R. X. *J. Controlled Release* **2006**, *116*, 266–274.
(24) Li, Y. Y.; Zhang, X. Z.; Kim, G. C.; Cheng, H.; Cheng, S. X.; Zhuo, R. X. *Small* **2006**, *2*, 917–923.
(25) Kohori, F.; Sakai, K.; Aoyagi, T.; Yokoyama, M.; Yamato, M.; Sakurai, Y.; Okano, T. *Colloids Surf., B* **1999**, *16*, 195–205.
(26) Liu, S. Q.; Tong, Y. W.; Yang, Y. Y. *Biomaterials* **2005**, *26*, 5064–5074.
(27) Liu, S. Q.; Tong, Y. W.; Yang, Y. Y. *Mol. Biosyst.* **2005**, *1*, 158–165.
(28) Nakayama, M.; Okano, T.; Miyazaki, T.; Kohori, F.; Sakai, K.; Yokoyama, M. *J. Controlled Release* **2006**, *115*, 46–56.
(29) Li, Y. Y.; Zhang, X. Z.; Cheng, H.; Zhu, J. L.; Li, U. N.; Cheng, S. X.; Zhuo, R. X. *Nanotechnology* **2007**, *18*, 505101.
(30) Loh, X. J.; Wu, Y. L.; Seow, W. T. J.; Norimzan, M. N. I.; Zhang, Z. X.; Xu, F. J.; Kang, E. T.; Neoh, K. G.; Li, J. *Polymer* **2008**, *49*, 5084–5094.
(31) Chang, C.; Wei, H.; Quan, C. Y.; Li, Y. Y.; Liu, J.; Wang, Z. C.; Cheng, S. X.; Zhang, X. Z.; Zhuo, R. X. *J. Polym. Sci., Part A: Polym. Chem.* **2008**, *46*, 3048–3057.
(32) Kohori, F.; Sakai, K.; Aoyagi, T.; Yokoyama, M.; Sakurai, Y.; Okano, T. *J. Controlled Release* **1998**, *55*, 87–98.
(33) Yamaoka, T.; Tabata, Y.; Ikada, Y. *J. Pharm. Sci.* **1994**, *83*, 601–606.
(34) Yamaoka, T.; Tabata, Y.; Ikada, Y. *J. Pharm. Sci.* **1995**, *84*, 349–354.
(35) Nakaoka, R.; Tabata, Y.; Yamaoka, T.; Ikada, Y. *J. Controlled Release* **1997**, *46*, 253–261.
(36) Jeong, B.; Bae, Y. H.; Kim, S. W. *Macromolecules* **1999**, *32*, 7064–7069.
(37) Jeong, B.; Bae, Y. H.; Kim, S. W. *Colloids Surf., B* **1999**, *16*, 185–193.
(38) Jeong, B.; Windisch, C. F., Jr.; Park, M. J.; Sohn, M. J.; Gutowska, A.; Char, K. *J. Phys. Chem. B* **2003**, *107*, 10032–10039.
(39) Lee, B. H.; Lee, Y. M.; Sohn, Y. S.; Song, S. C. *Macromolecules* **2002**, *35*, 3876–3879.
(40) Astafieva, I.; Zhong, X. F.; Eisenberg, A. *Macromolecules* **1993**, *26*, 7339–7352.
(41) Wilhelm, M.; Zhao, C.; Wang, Y.; Xu, R.; Winnik, M. A.; Mura, J. L.; Riess, G.; Croucher, M. D. *Macromolecules* **1991**, *24*, 1033–1040.
(42) Li, J.; Ni, X. P.; Li, X.; Tan, N. K.; Lim, C. T.; Ramakrishna, S.; Leong, K. W. *Langmuir* **2005**, *21*, 8681–8685.
(43) Li, X.; Mya, K. Y.; Ni, X.; He, C.; Leong, K. W.; Li, J. *J. Phys. Chem. B* **2006**, *110*, 5920–5926.
(44) Chang, Y.; Lee, S. C.; Him, K. T.; Him, C.; Reeves, S. D.; Allcock, H. R. *Macromolecules* **2001**, *34*, 269–274.
(45) Allcock, H. R.; Cho, S. Y.; Steely, L. B. *Macromolecules* **2006**, *39*, 8334–8338.
(46) Lee, S. C.; Chang, Y. K.; Yoon, J. S.; Kim, C. H.; Kwon, I. C.; Kim, Y. H.; Jeong, S. Y. *Macromolecules* **1999**, *32*, 1847–1852.
(47) Xu, J.; Ye, J.; Liu, S. *Macromolecules* **2007**, *40*, 9103–9110.
(48) Fujishige, S.; Kubota, K.; Ando, I. *J. Phys. Chem.* **1989**, *93*, 3311–3313.
(49) Yamamoto, I.; Iwasaki, K.; Hirotsu, S. *J. Phys. Soc. Jpn.* **1989**, *58*, 210–215.

MA8019865